

# Feedback effects of boundary-layer meteorological factors on cumulative explosive growth of PM<sub>2.5</sub> during winter heavy pollution episodes in Beijing from 2013 to 2016

Junting Zhong<sup>1</sup>, Xiaoye Zhang<sup>1, 2</sup>, Yunsheng Dong<sup>3</sup>, Yaqiang Wang<sup>1</sup>, Cheng Liu<sup>2, 3, 4</sup>, Jizhi Wang<sup>1</sup>, Yangmei Zhang<sup>1</sup>, Haochi Che<sup>5</sup>

<sup>1</sup>State Key Laboratory of Severe Weather & Key Laboratory of Atmospheric Chemistry of CMA, Chinese Academy of Meteorological Sciences, China.

<sup>2</sup>Center for Excellence in Regional Atmospheric Environment, IUE, Chinese Academy of Sciences, China.

<sup>3</sup>Key Laboratory of Environmental Optics and Technology, Anhui Institute of Optics and Fine Mechanics, Chinese Academy of Sciences, China.

<sup>4</sup>School of Earth and Space Sciences, University of Science and Technology of China, Hefei 230026, China

<sup>5</sup>Department of Physics, University of Oxford, UK.

*Correspondence to:* X.Y. Zhang (xiaoye@camsma.cn)

**Abstract.** In January of 2013, February of 2014, December of 2015, and December of 2016 to January 10<sup>th</sup> of 2017, 12 persistent heavy aerosol pollution episodes (HPEs) occurred in Beijing, which has attracted special attention from the public. During the HPEs, the precise cause of PM<sub>2.5</sub> explosive growth (mass concentration at least doubled in several to ten hours) is uncertain. Here, we analyzed and estimated relative contributions of boundary-layer meteorological factors to such growth, using ground and vertical meteorological data. Beijing HPEs are generally characterized by the transport stage (TS), whose aerosol pollution formation is primarily caused by pollutants transported from the south of Beijing, and the cumulative stage (CS), in which the cumulative explosive growth of PM<sub>2.5</sub> mass is dominated by stable atmospheric stratification characteristic of southerly slight or calm winds, near-ground anomalous inversion, and moisture accumulation. During the CSs, observed southerly weak winds facilitate local pollutant accumulation by minimizing horizontal pollutant diffusion. Established from TSs, elevated PM<sub>2.5</sub> levels scatter more solar radiation back to the space to reduce near-ground temperature, which very likely causes anomalous inversion. This surface cooling by PM<sub>2.5</sub> decreases near-ground saturation vapor pressure and increases relative humidity significantly; the inversion subsequently reduces vertical

31 turbulent diffusion and boundary layer height to trap pollutants and accumulate water vapor. Appreciable  
32 near-ground moisture accumulation ( $RH > 80\%$ ) would further enhance aerosol hygroscopic growth and  
33 accelerate liquid-phase and heterogeneous reactions, in which incompletely quantified chemical  
34 mechanisms need more investigation. Noted positive meteorological feedback on  $PM_{2.5}$  mass explains  
35 over 70% of cumulative explosive growth.

36

37 **Keyword:** Southerly transport; anomalous inversion; moisture accumulation; meteorological feedback.

38

## 39 1 Introduction

40 Since a persistent heavy fog and haze event occurred in eastern China in January 2013, fine  
41 particulate matter smaller than 2.5  $\mu\text{m}$  in diameter ( $\text{PM}_{2.5}$ ), as a key component of pollution episodes,  
42 has drawn wide attention all over China. Elevated  $\text{PM}_{2.5}$  leads a sharp decrease in visibility that affects  
43 economic activities by causing traffic disruptions and contains toxic substances that affect respiratory  
44 and circulatory system (Chen et al., 2013; Bai et al., 2007). The interaction between aerosol and radiation  
45 directly and indirectly affects weather and climate (Zhang et al., 2013; Zhang et al., 2015b; Wei et al.,  
46 2011; Boucher et al., 2013; Wang et al., 2010). China has experienced heavy aerosol pollution episodes  
47 recently, with  $\text{PM}_{2.5}$  reaching unprecedentedly high levels in many cities, particularly Beijing and its  
48 vicinity (BIV), which is one of the nation's most polluted regions (Zhang et al., 2012).

49 To elucidate the causes of such heavy pollution episodes, a variety of explanations have been  
50 proposed (Huang et al., 2014; Sun et al., 2014a; Sun et al., 2014b; Wang et al., 2014b; Wang et al.,  
51 2014c). Previous studies found that atmospheric conditions represented one critical parameter in  
52 regulating the cycles of pollution episodes in Beijing in autumn 2013 (Guo et al., 2014; Zhang et al., 2009)  
53 and in the North China Plain and other areas in China (Zhang et al., 2015c). During one pollution episode,  
54 an analysis of atmospheric background fields revealed dynamic and thermodynamic effects substantially  
55 affected pollution formation (Zhang et al., 2014). Specifically, aerosol pollution in Beijing was possibly  
56 contributed by southerly/southwesterly surface wind (Wang et al., 2013b). This likely attribution was  
57 further verified by source apportionment from the Beijing Environmental Protection Bureau in  
58 2012~2013. In addition, aerosol pollution can be formed by secondary aerosol formation through  
59 atmospheric chemical reactions, including liquid-phase reactions, in which aqueous  $\text{SO}_2$  is oxidized by  
60  $\text{NO}_2$ ,  $\text{H}_2\text{O}_2$  and  $\text{O}_3$  to form sulfate, and heterogeneous reactions, in which  $\text{NO}_2$  and  $\text{N}_2\text{O}_5$  form nitrates  
61 with water (Zheng et al., 2015a; Cheng et al., 2016).

62 Although these cited studies existed, the formation mechanism during different stages for heavy  
63 aerosol pollution in Beijing, especially the explosive growth stage of  $\text{PM}_{2.5}$  mass concentration, is still  
64 not clear. Previous studies focused more on whether unfamiliar chemical mechanisms were not or  
65 inadequately considered in Beijing, a region with high concentrations of various aerosol components

66 (Wang et al., 2014b). This view was questioned by subsequent research, suggesting that such rapid  
67 growth is mainly attributable to the regional transport of clean and polluted air mass, which derived from  
68 the comparison between surface meteorological factors and the PM<sub>2.5</sub> mass concentration in several cities  
69 of the North China Plain (Zheng et al., 2015b). However, the attribution of such growth's drivers is  
70 unreasonable occasionally, because the rapid growth may occur with weak surface winds and stable  
71 stratification, which are unfavorable for transport. Then vertical meteorological variations in the  
72 boundary layer (BL) in one autumnal episode have been analyzed, which significantly affect the PM<sub>2.5</sub>  
73 mass concentration near the ground (Hua et al., 2016). However, in the absence of long-term observations  
74 of meteorological factors and pollutant concentrations, most research concerning pollution causes  
75 focuses on one or several consecutive pollution episodes in a certain time, and almost no research attempt  
76 to investigate, conclude and quantify the contributions of meteorological factors to the majority of heavy  
77 pollution episodes since 2013, particularly the feedback effect of meteorological factors during explosive  
78 growth processes. Such investigations will definitely provide a clearer understanding of roles that various  
79 vertical meteorological factors play in heavy pollution episodes. Therefore, this paper primarily uses  
80 vertical measurements of meteorological factors in the BL from 2013 to 2016, investigates their  
81 contributions to the explosive growth of PM<sub>2.5</sub> during the heavy pollution episodes in Beijing, and also  
82 attempts to quantify the effect of meteorological factors on the explosive growth of PM<sub>2.5</sub> levels.  
83

84 **2 Methods**

85 In this study, the following data are used. (1) Hourly PM<sub>2.5</sub> mass concentration measured by state-  
86 controlled stations of the Ministry of Environmental Protection in Beijing and Baoding. PM<sub>2.5</sub> mass  
87 concentrations of urban stations were averaged to represent urban pollution conditions. (2) Atmospheric  
88 vertical observations twice daily at 0800 Beijing Time (BJT) and 2000 BJT, including winds, temperature  
89 and relative humidity (RH), measured using L-band radiosonde radar at the observatory (54511) in  
90 southern Beijing from 1 January 2013 to 31 January 2013, 1 February 2014 to 28 February 2014, 26  
91 November 2015 to 31 December 2015 and 21 December 2016 to 10 January 2017. The observatory is  
92 located on the edge of urban area of Beijing, so it could be used to represent urban vertical meteorological  
93 conditions to some degree due to the regional change characteristics of air masses. (3) Hourly ground-  
94 level meteorological observations from automatic weather stations (AWSs) provided by the National  
95 Meteorological Information Center of the China Meteorological Administration. (4) Lidar observations  
96 were measured every fifteen minutes by one Mie-elastic backscatter polarization lidar emitting short  
97 pulses of 20 Hz at 532nm in the Institute of Atmospheric Physics, located in the northern urban area of  
98 Beijing. The optical parameters of the aerosol particles were retrieved by the backscattering signals. Then  
99 the vertical profiles of the aerosol extinction coefficient and linear depolarization ratio were obtained  
100 based on the assumptive lidar ratios as 50 for aerosols using the Fernald's method (Fernald, 1984;Lv et  
101 al., 2017). (5) A parameterized index, PLAM (Parameter Linking Aerosol Pollution and Meteorological  
102 Elements), calculated with the observations from the observatory (54511). PLAM was built as a function  
103 of the following parameters:

104 
$$\text{PLAM}(F) \in f(p, t, w, rh, e, s, c', \dots) \quad (1)$$

105 where p, t, w, rh, e, s, and c' represent air pressure, air temperature, winds, relative humidity,  
106 evaporability, stability, and effective parameter associated with the contribution of air pollution  $\beta(c')$ ,  
107 respectively. Plam is further attributed to two major separate factors: (1) initial meteorological conditions  
108  $\alpha(m)$  associated with the atmospheric condensation processes and (2) a dynamic effective parameter  
109 associated with the initial contribution of air pollution  $\beta(c')$  :

110 
$$\text{PLAM} = \alpha(m) \times \beta'(c). \quad (2)$$

111 It mainly indicates the regional atmospheric stability and air condensation ability. The details of its  
112 calculation are presented in previous studies (Wang et al., 2013a;Zhang et al., 2015c;Zhang et al.,  
113 2009;Wang et al., 2012).

### 114 **3 Results and discussion:**

#### 115 *3.1 Characteristics of explosive growth in HPEs*

116 A period during which the PM<sub>2.5</sub> level is less than 35 µg m<sup>-3</sup> is defined as a clean period based on  
117 the PM<sub>2.5</sub> daily mean mass concentration limit in the primary standard of China's national environmental  
118 quality standards, while a pollution episode is referred to as an episode during which the PM<sub>2.5</sub> exceeds  
119 80 µg m<sup>3</sup> for 3 consecutive days between two clean periods. Pollution episodes with peak PM<sub>2.5</sub> values  
120 less than 300 µg m<sup>-3</sup> or more than 400 µg m<sup>-3</sup> are termed light pollution episodes (LPEs) or heavy  
121 pollution episodes (HPEs), respectively.

122 Based on the urban PM<sub>2.5</sub> monthly mean mass concentration in winter Beijing from 2013 to 2016,  
123 the months with highest mass concentration each year were selected to represent the severe PM<sub>2.5</sub>  
124 pollution conditions in winter, which are January in 2013, February in 2014, December in 2015 and  
125 December in 2016 respectively. These months are termed the wintertime pollution period (WPP) for the  
126 convenience of further investigation.

127 During the WPP, 12 HPEs occur in total (Fig. 1~4 (dark gray)), whose PM<sub>2.5</sub> mass concentration is  
128 244.3 µg m<sup>-3</sup> on average. The maximum mean value (307.4 µg m<sup>-3</sup>) appears in HPE<sub>1</sub>, which has been  
129 analyzed in detail in a variety of papers (Zhang et al., 2013;Zhang et al., 2014). The concentrations of  
130 HPE<sub>6</sub> and HPE<sub>10</sub> are 304.2 µg m<sup>-3</sup> and 294.5 µg m<sup>-3</sup> respectively, which are slightly lower than HPE<sub>1</sub>.  
131 The minimum mean concentration of PM<sub>2.5</sub> occurs in HPE<sub>8</sub> (160.4 µg m<sup>-3</sup>), which is nearly twice as much  
132 as the mean annual mass concentration of PM<sub>2.5</sub> in 2015, nevertheless.

133 Typical PM<sub>2.5</sub> rising processes (color-mark) in HPEs were selected, which appeared in 11 of the 12  
134 HPEs. The green-mark processes are tentatively referred to as rising processes, since they generally keep  
135 rising consistently with relatively strong southerly winds compared with subsequent growth and vary  
136 sensitively and rapidly in response to wind shift from northerly to southerly in the BL. During HPEs, the

137 growth processes in which the PM<sub>2.5</sub> mass concentration is at least doubled in several or ten hours in the  
138 later period of HPEs are termed explosive growth processes. The red-mark explosive growth processes  
139 are tentatively termed cumulative explosive growth processes because of anomalous inversion  
140 facilitating pollutant accumulation. The purple-mark explosive growth processes are tentatively known  
141 as convergent explosive growth processes, for local wind convergence occurs (Fig. 6) with weak wind  
142 velocity and no anomalous inversion. The early stages of HPEs during which PM<sub>2.5</sub> keeps rising are  
143 defined as transport stages (TSs), while the later stages during which cumulative/convergent explosive  
144 growth appears are termed cumulative stages (CSs).

### 145 **3.2 Meteorological causes of the explosive growth in HPEs**

#### 146 **3.2.1 PM<sub>2.5</sub> pollution formation is primarily caused by pollutants transported from the south of** 147 **Beijing, which subsequently worsen weather conditions**

148 We found that during clean periods occur mostly strong northwesterly winds whose velocity  
149 increases with height; during the HPEs, the southwesterly winds with dramatically decreased velocity  
150 were most frequent (Fig. 1-4 (a, b)). Strong northerly winds and weak southerly winds closely correspond  
151 to the clean periods and the HPEs respectively, because northwesterly winds, which are from less  
152 populated north mountainous areas, carry unpolluted air masses while southerly winds carry polluted air  
153 masses from more populated and polluted southern industrial regions (Jia et al., 2008; Liu et al., 2013; Guo  
154 et al., 2014).

155 During the TSs with southerly winds, air temperature and moisture substantially increase compared  
156 with clean periods with northerly winds (Fig. 1-4 (b, c, d)), which indicates warm and humid southerly  
157 airflow transport more water vapor and heat into Beijing. During 15 rising processes ((green lines)),  
158 nearly no striking near-ground (<250m) moisture accumulation appears; no anomalous inversion appears  
159 except brief weak inversion, which suggest that vertical variations of temperature and RH are unlike to  
160 primarily cause such rising. Nevertheless, weak inversion and more near-ground moisture favor growth.

161 If we assume that the primary cause of this rising is pollution accumulation due to local emissions,  
162 the rising needs to coincide with light (0.3~1.5 m s<sup>-1</sup>) or calm (0~0.2 m s<sup>-1</sup>) air observed during the later

163 TSs instead of slight ( $1.6\sim 3.3\text{ m s}^{-1}$ ) or gentle ( $3.4\sim 5.4\text{ m s}^{-1}$ ) breeze observed during the early TSs,  
164 because weaker winds result in a stagnant condition, which is more favorable for local accumulation.

165 However, the majority of later TSs with calm air do not exhibit such rising (Fig. 1-4 (a, b)), which  
166 suggests local emissions under weak winds are likely conducive but not dominant with respect to rising.

167 Before rising processes during HPE<sub>1~2</sub>, the urban PM<sub>2.5</sub> mass concentration of Baoding (light gray  
168 lines), which is typically representative of pollution conditions in the south of Beijing, was much higher  
169 than Beijing; the winds in Beijing rapidly shifted from northerly to southerly. Then the rising (green lines)  
170 occurred, consistently with southerly slight or gentle breezes in the BL (green boxes). The southerly air  
171 mass move more than  $288\text{ km d}^{-1}$  below 500 m (estimated from the measured wind speed), which are fast  
172 enough to transport pollutants to Beijing. Similar conditions appeared in 8 of other 9 HPEs with rising.  
173 Such processes indicate southerly pollutant transport is primarily responsible for the rising, given the  
174 pollution transport pathway of the southwest wind belt determined by the unique geographic features of  
175 the North China Plain, with the Tai-hang Mountains and the Yan Mountains strengthening the southwest  
176 wind belt and leading the convergence of pollutant transport in Beijing. (Su et al., 2004). Governed by  
177 this transport pathway, PM<sub>2.5</sub> mass concentration increased by  $\sim 400\text{ }\mu\text{g m}^{-3}$  from less than  $35\text{ }\mu\text{g m}^{-3}$  in  
178 ten hours on 22 January 2013, when winds shifted from northerly to southerly with much higher PM<sub>2.5</sub>  
179 concentrations in Baoding.

180 Pollutants transported from the south of Beijing primarily results in PM<sub>2.5</sub> pollution formation in the  
181 urban Beijing area, to which possible weak inversion and the near-surface moisture accumulation is  
182 conducive. Warm and humid airflow from the south transports more water vapor and pollutants to the  
183 North China Plain, which creates the requisite moisture and pollution accumulation conditions for  
184 subsequently cumulative explosive growth.

### 185 **3.2.2 Worsening meteorological conditions primarily cause cumulative explosive growth**

#### 186 *Feedback of anomalous inversion on pollutant accumulation*

187 Anomalous inversion occurs during 10 of 12 HPEs (Fig. 1~4 (a, c)). The factors that cause inversion  
188 in Beijing includes topography, advection and radiation. With the Tai-hang Mountains and the Yan



189 Mountains lying north of Beijing, a cold air mass flows down into the urban of Beijing from the mountain  
190 peaks, which occasionally causes topography inversion; advection inversion occurs when a warm and  
191 less dense air mass moves over a cold and dense air mass. However, during most cumulative stages, the  
192 anomalous inversion appears with slight or calm winds, which suggests that the movement of air masses  
193 is not striking, so the contribution of topography and advection to such inversion is limited. The ground  
194 emits long-wave radiation at night to reduce near-ground temperature to facilitate inversion occasionally.  
195 However, almost no anomalous inversion occurs without pre-existing high PM<sub>2.5</sub> mass concentration in  
196 the WPP (Fig. 1~4), which suggests that the ground radiation are likely conducive to weak/normal  
197 inversion, but not dominant with respect to anomalous inversion.

198 Noted anomalous inversion is preceded by existing relatively high PM<sub>2.5</sub> levels generally established  
199 by the rising processes. Before the cumulative explosive growth, existing aerosols are concentrated  
200 below 500 m (Fig. 5). These low-layer aerosols back-scatter amounts of radiation to space (Wang et al.,  
201 2014a;Gao et al., 2015), and cause a significant reduction in radiation reaching the ground, which further  
202 reduces near-ground temperature. These findings indicate that anomalous inversion is primarily due to  
203 radiation cooling effect of pre-existing aerosols. Below the inversion, near-ground temperature reduction  
204 cools down plumes or thermals of originally warm surface air to decrease thermal turbulence; observed  
205 weakened vertical shear of horizontal winds (Fig. 1~4 (b)) produces less vorticity to reduce mechanical  
206 turbulence, which further strengthens the existing inversion.

207 Anomalous inversion traps pollution-laden air beneath it due to its strong static stability (Wallace  
208 and Hobbs, 2006). It facilitates pollutant accumulation by suppressing vertical air mixing and reducing  
209 BL height. During the cumulative explosive growth with anomalous inversion in the HPE<sub>10</sub>, the turbulent  
210 diffusion coefficient rapidly decreases from 100 m<sup>2</sup> s<sup>-1</sup> to 50 m<sup>2</sup> s<sup>-1</sup> (model output of CUACE/Chem, the  
211 meso-scale China Meteorological Administration (CMA) Unified Atmospheric Chemistry modelling  
212 system, personal communication with Dr. Hong Wang), and similar conditions of turbulent diffusion  
213 have been modelled in another pollution episode in Beijing (Wang et al., 2015a;Wang et al., 2015b); the  
214 BL height decreases from ~500 m in the early morning, to ~350 m at noon, even to ~250 m at night (Fig.  
215 5), which coincide with the increase of PM<sub>2.5</sub> from ~200 to ~450 µg m<sup>-3</sup> (Fig. 4 (a)). The striking layered  
216 structure in the BL occurs at the height of ~300 m on 20 December 2016 (Fig. 5), which is consistent

217 with the lower edge of anomalous inversion (Fig. 4), which verifies the strong inhibition of anomalous  
218 inversion. Additionally, a short cold air mass invades the northern urban area of Beijing in the early  
219 morning on 20 December 2016. The enhanced movement increases the BL height and reduces the PM<sub>2.5</sub>  
220 mass concentration in part of northern urban area (Fig. 5), which slightly reduces the urban mean mass  
221 concentration of PM<sub>2.5</sub> (Fig. 4 (1)). However, the anomalous inversion rapidly restores its original  
222 structure to facilitate pollutant accumulation.

223 The occurrence of anomalous inversion in 9 HPEs coincides with cumulative explosive growth of  
224 PM<sub>2.5</sub> levels (F1~4 (a, c)), which verifies the suppression of anomalous inversion to pollutants. Note that  
225 no cumulative explosive growth of PM<sub>2.5</sub> levels appears in HPE<sub>3</sub> despite anomalous inversion, partly  
226 because the height of the lowest inversion layer in HPE<sub>3</sub> (~750 m) is much higher than that in the 9 HPEs  
227 (~ 250 meters), which suggests near-ground inversion is more favorable for pollutant accumulation.

#### 228 *Anomalous inversion results in near-surface moisture accumulation*

229 During clean periods, the moisture is evenly distributed in the BL with RH less than 40%, while  
230 during the HPEs, RH is over 60% (even 80%) in the lower or upper BL (Fig. 1~4 (c, d)). During the  
231 HPEs, in the absence of temperature inversion, moisture vertically distributes in the BL, and the RH in  
232 the upper BL is occasionally higher than that of the near-ground surface; in the presence of weak  
233 inversion, the lower edge of the inversion layer is in approximate agreement with the RH contour of 60%;  
234 In the presence of anomalous inversion (red boxes in Fig. 1~4 (c)) in the BL, the lower edge of the strong  
235 inversion layer frequently coincides with an RH contour of 80% (red boxes in Fig. 1~4 (d)), which is  
236 observed in most cumulative explosive growth processes.

237 The previously noted relation of vertical temperature and RH indicates that anomalous inversion  
238 results in appreciable near-surface moisture accumulation by suppressing the vertical mixing of the water  
239 vapor (Wallace and Hobbs, 2006). The vertical diffusion of the near-surface water vapor as the anomalous  
240 inversion disappeared on 1 December 2016, 26 December 2016, and 5 January 2017 verifies the cited  
241 research outcome. Noted that mentioned near-ground temperature reduction caused by cooling effects of  
242 aerosols is also conducive to moisture accumulation by decreasing near-ground saturation vapor pressure  
243 to increase RH.

244 *Moisture accumulation facilitates aerosol hygroscopic growth and additional secondary aerosol*  
245 *formation*

246 Strong absorbent aerosol particles absorb and grow, when additional water vapor appears in the air  
247 (Zhang et al., 2015a). The mass concentrations of organic aerosols, sulfate, nitrate, and ammonium  
248 rapidly increase with RH (Fig. S1). After moisture absorption in North China, aerosol particle size  
249 increases 20%~60% (Pan et al., 2009) and aerosol direct radiative forcing increases ~50% (Zhang et al.,  
250 2015a). As a key component of atmospheric aerosols, aerosol water serves as a medium that enables  
251 aqueous-phase reactions (Pilinis et al., 1989; Seinfeld and Pandis, 1986; Ervens et al., 2011). For example,  
252 aerosol water serves as a reactor in which alkaline aerosol components trap SO<sub>2</sub>, which is then oxidized  
253 by NO<sub>2</sub> to form sulfate in northern China (Cheng et al., 2016). The ratio of SO<sub>2</sub> to SO<sub>4</sub><sup>2-</sup> ranges from less  
254 than 0.1 at relative humidity (RH) <20% to 1.1 at RH >90%, exhibiting an exponential increase with RH  
255 (Wang et al., 2016). In addition, high RH facilitates heterogeneous chemical processes to aggravate air  
256 pollution (Zhu et al., 2011). For example, the net reaction probability of HNO<sub>3</sub> uptake on CaCO<sub>3</sub> particles  
257 was found to increase with relative humidity from ~0.003 at 10% to 0.21 at 80% (Liu et al., 2008).

258 *Stable atmospheric stratification characteristic of southerly light or calm winds, anomalous inversion,*  
259 *and near-ground (<250 m) moisture accumulation (RH>80%) dominates the cumulative explosive*  
260 *growth of PM<sub>2.5</sub>.*

261 During the HPEs, nearly all 10 cumulative explosive growth processes (Fig. 1-4) occur concurrently  
262 with stable atmospheric stratification primarily characterized by southerly light or calm winds, near-  
263 ground anomalous inversion, and cumulative moisture (RH>80%). The weak southerly winds increased  
264 with height are conducive to the growth, because relatively strong southerly winds in the upper BL  
265 (~1000m) transport pollutants from the south of Beijing, while low-level (~250m) southerly light or calm  
266 winds limiting the invasion of northerly cold winds facilitates local pollution accumulation by  
267 minimizing horizontal pollutant diffusion. The anomalous inversion facilitates vertical pollutant  
268 accumulation by suppressing convection activities. During the cumulative growth process in HPE<sub>10</sub>, the  
269 turbulent diffusion coefficient rapidly decreases from 100 m<sup>2</sup> s<sup>-1</sup> to 50 m<sup>2</sup> s<sup>-1</sup> and the BL height decreases

270 from 500 m to ~250 m, which is extremely favorable for pollutants accumulation. Additional suppression  
271 of vertical mixing of water by inversion and previously noted decreased saturation vapor pressure cause  
272 near-surface moisture accumulation (RH>80%). This accumulated moisture facilitates secondary aerosol  
273 formation in liquid-phase and heterogeneous reactions to increase PM<sub>2.5</sub> levels.

274 It's likely that merely weak southerly winds or near-ground anomalous inversion primarily can  
275 cause cumulative explosive growth. However, the growth does not occur in the polluted process from 4  
276 to 15 December 2015 with weak southerly winds, which indicates that weak southerly winds do not  
277 suffice to cause cumulative explosive growth in the absence of anomalous inversion; even with  
278 anomalous inversion, no explosive growth appeared on 14 and 24 January 2013, which suggests that  
279 anomalous inversion cannot cause explosive growth without weak southerly winds. Therefore,  
280 cumulative explosive growth in CSs is primarily resulted from the joint effects of southerly light or calm  
281 winds, near-ground anomalous inversion and moisture accumulation.

282 Note that the cumulative explosive growth at 2000 BJT on 3 January was accompanied by a  
283 southerly gentle breeze (3.4~5.4 m s<sup>-1</sup>), which suggests that low-level southerly pollutant transport  
284 occasionally exerts an important impact on the growth, with anomalous inversion and near-ground  
285 moisture accumulation.

#### 286 *Feedback of cumulative pollutants on worsening meteorological conditions*

287 Established from cumulative explosive growth, exceedingly high PM<sub>2.5</sub> levels further decrease the  
288 near-ground temperature by reflecting and scattering more solar radiation, which strengthens the existing  
289 anomalous inversion and subsequently results in additional pollutant accumulation until the next synoptic  
290 process occurs. The near-surface temperature decreased from 3°C at 2000 BJT on 19 December to -3°C  
291 at 0800 BJT on 20 December after elevated ground PM<sub>2.5</sub> levels (Fig. 4 (d)). Then it had remained at ~-  
292 1°C with PM<sub>2.5</sub> of more than 400 µg m<sup>-3</sup> over the next 2 d until northerly strong and clean winds blew  
293 the pollution away on 22 December. Similar processes also occurred in the CSs of other HPEs, which  
294 verifies the outcome.

### 295 **3.2.3 Local air convergence is favorable for convergent explosive growth.**

296 The explosive growth of  $PM_{2.5}$  appears in  $HPE_{4-5}$  without inversion and near-ground moisture  
297 accumulation (Fig. 2), which suggests previously noted stable atmospheric stratification does not  
298 primarily cause the growth. Weak winds in convergent explosive growth processes, particularly the  
299 process in  $HPE_5$ , eliminate the likely contributions of southerly transport pollution. A comparison of  
300 surface wind distributions in the North China Plain before (Fig. 6 (a, d)) and during (Fig. 6 (b, c; d, e))  
301 the convergent explosive growth processes in  $HPE_{4-5}$  shows that the urban area of Beijing is dominated  
302 by northerly winds before the growth, while is characterized by local air convergence during the  
303 processes, which suggests that the persistent local convergence is conducive to the explosive growth by  
304 causing pollutants to further locally accumulate. The convergent explosive growth in  $HPE_{6-7}$  with air  
305 convergence (Fig. S2) also verifies the outcome.

### 306 **3.3 Quantification of meteorological contributions to $PM_{2.5}$ cumulative explosive growth**

307 Cooling effects of elevated  $PM_{2.5}$  levels established from TSs worsen meteorological conditions,  
308 which primarily causes cumulative explosive growth. To approximately quantify this atmospheric  
309 feedback on the growth, PLAM (Parameter Linking Aerosol Pollution and Meteorological Elements)  
310 was used, which was derived from the relationship of  $PM_{2.5}$  with key meteorological parameters. The  
311 PLAM index, whose details of calculation have been described in Wang et al. (Wang et al., 2013a; Wang  
312 et al., 2012), primarily reflects the stability of the air mass and the condensation rate of water vapor on  
313 aerosol particles. It has been employed to identify the contribution of specific meteorological factors to  
314 a 10 d haze–fog event in 2013 (Zhang et al., 2013) and to evaluate the contribution of meteorological  
315 factors to changes in atmospheric composition and optical properties over Beijing during the 2008  
316 Olympic Games (Zhang et al., 2009). During cumulative explosive growth processes, the hourly  
317 variation of urban mean  $PM_{2.5}$  mass concentration is in closely linear agreement with that of PLAM for  
318 Beijing (Fig. 7 (a~d)). The squared correlation coefficients between hourly PLAM and  $PM_{2.5}$  in 2013,  
319 2015, and 2016 are 0.71, 0.69, and 0.71 respectively, exceeding the 0.05 significance level. The mean  
320 value of four coefficients is over 0.70, which suggests the noted feedback of worsening meteorological

321 conditions on PM explains over 70% in cumulative explosive growth of  $PM_{2.5}$ . In addition, the squared  
322 correlation coefficients between PLAM and  $PM_{2.5}$  in 2014 is 0.76, which indicates enhanced regional  
323 atmospheric stability facilitate convergent explosive growth of  $PM_{2.5}$ .

#### 324 **4 Conclusion:**

325 We have characterized different stages of 12 HPEs during the WPP (wintertime pollution periods)  
326 in Beijing and typical explosive growth of  $PM_{2.5}$ , including cumulative and convergent explosive growth.  
327 Meteorological causes to such growth are elucidated, based on observations of vertical meteorological  
328 factors within the BL (Fig. 8). Beijing HPEs can generally be divided into the TS, whose rising processes  
329 is primarily caused by pollutants transported from south of Beijing, and the CS, in which stable  
330 atmospheric stratification dominates the cumulative explosive growth of  $PM_{2.5}$ .

331 Polluted and humid airflow from the south of Beijing transports water vapor and pollutants to  
332 Beijing, which primarily causes rising processes and creates the requisite moisture and pollution  
333 accumulation conditions for CSs. Elevated  $PM_{2.5}$  levels established from the TS reduce near-ground  
334 temperature by back scattering short-wave solar radiation. This temperature reduction very likely results  
335 in anomalous inversion, which is enhanced by the reduced mechanical turbulence that results from less  
336 vorticity caused by observed weakened vertical shear of horizontal winds in the lower BL during the later  
337 TSs and decreased thermal turbulence with cooling plumes or thermals of originally warm surface air  
338 that result from the decreased near-ground temperature. Anomalous inversion reduces turbulent diffusion  
339 and decreases the BL height to trap pollutants. The similar suppression of anomalous inversion to vertical  
340 mixing of water vapor and decreased saturation water vapor pressure caused by noted temperature  
341 reduction result in appreciable near-surface moisture accumulation ( $RH > 80\%$ ). The accumulated  
342 moisture facilitates pollutant accumulation by enhancing hygroscopic growth and accelerating liquid-  
343 phase and heterogeneous reactions. However, specific reaction mechanisms have not been fully  
344 quantified and require additional investigation, particularly their contributions to the explosive growth  
345 and the maintenance of  $PM_{2.5}$  during CSs. Note that observed southerly weak winds facilitate local  
346 pollutant accumulation by minimizing horizontal pollutant diffusion. The joint effects of southerly weak  
347 winds, near-ground anomalous inversion, and moisture accumulation dominate cumulative explosive

348 growth of PM<sub>2.5</sub>. Nearly 70% of the growth is attributable to noted meteorological feedback, based on  
349 correlation analysis between PM<sub>2.5</sub> and PLAM index during cumulative explosive growth processes.  
350 Note that sporadic local air convergence also causes pollutants to further accumulate.

351 Established from cumulative explosive growth, exceedingly high PM<sub>2.5</sub> levels further decrease the  
352 near-ground temperature to strengthen the existing anomalous inversion, which results in additional  
353 pollutant accumulation until the next synoptic process occurs.

## 354 **References**

- 355 Bai, N., Khazaei, M., van Eeden, S. F., and Laher, I.: The pharmacology of particulate matter air  
356 pollution-induced cardiovascular dysfunction, *Pharmacology & Therapeutics*, 113, 16, 2007.
- 357 Boucher, O., Randall, D., Artaxo, P., Bretherton, C., Feingold, G., Forster, P., Kerminen, V. V. M.,  
358 Kondo, Y., Liao, H., Lohmann, U., Rasch, P., Satheesh, S. K., Sherwood, S., Stevens, B., and  
359 Zhang, X. Y.: Clouds and Aerosols, in: *Climate Change 2013: The Physical Science Basis. Contribution of Working Group I to the Fifth Assessment Report of the Intergovernmental Panel on Climate Change*, edited by: Stocker, T. F., Qin, D., Plattner, G.-K., Tignor, M., Allen, S. K., Boschung, J., Nauels, A., Xia, Y., Bex, V., and Midgley, P. M., Cambridge University Press, Cambridge, United Kingdom and New York, NY, USA, 571-658, 2013.
- 364 Chen, Y., Ebenstein, A., Greenstone, M., and Li, H.: Evidence on the impact of sustained exposure  
365 to air pollution on life expectancy from China's Huai River policy, *Proceedings of the National Academy of Sciences of the United States of America*, 110, 12936-12941, 10.1073/pnas.1300018110, 2013.
- 368 Cheng, Y., Zheng, G., Chao, W., Mu, Q., Bo, Z., Wang, Z., Meng, G., Qiang, Z., He, K., and  
369 Carmichael, G.: Reactive nitrogen chemistry in aerosol water as a source of sulfate during haze  
370 events in China, *Science Advances*, 2, 2016.
- 371 Ervens, B., Turpin, B. J., and Weber, R. J.: Secondary organic aerosol formation in cloud droplets  
372 and aqueous particles (aqSOA): a review of laboratory, field and model studies, *Atmospheric Chemistry and Physics*, 11, 11069-11102, 10.5194/acp-11-11069-2011, 2011.
- 374 Fernald, F. G.: Analysis of atmospheric lidar observations: some comments, *Applied Optics*, 23, 652,  
375 1984.
- 376 Gao, Y., Zhang, M., Liu, Z., Wang, L., Wang, P., Xia, X., Tao, M., and Zhu, L.: Modeling the  
377 feedback between aerosol and meteorological variables in the atmospheric boundary layer  
378 during a severe fog-haze event over the North China Plain, *Atmospheric Chemistry and Physics*, 15, 4279-4295, 10.5194/acp-15-4279-2015, 2015.
- 380 Guo, S., Hu, M., Zamora, M. L., Peng, J. F., Shang, D. J., Zheng, J., Du, Z. F., Wu, Z., Shao, M.,  
381 Zeng, L. M., Molina, M. J., and Zhang, R. Y.: Elucidating severe urban haze formation in China,  
382 *Proceedings of the National Academy of Sciences of the United States of America*, 111, 17373-  
383 17378, 10.1073/pnas.1419604111, 2014.

384 Hua, Y., Wang, S., Wang, J., Jiang, J., Zhang, T., Song, Y., Kang, L., Zhou, W., Cai, R., Wu, D., Fan,  
385 S., Wang, T., Tang, X., Wei, Q., Sun, F., and Xiao, Z.: Investigating the impact of regional  
386 transport on PM<sub>2.5</sub> formation using vertical observation during APEC 2014 Summit in Beijing,  
387 *Atmospheric Chemistry and Physics*, 16, 15451-15460, 10.5194/acp-16-15451-2016, 2016.

388 Huang, R.-J., Zhang, Y., Bozzetti, C., Ho, K.-F., Cao, J.-J., Han, Y., Daellenbach, K. R., Slowik, J.  
389 G., Platt, S. M., and Canonaco, F.: High secondary aerosol contribution to particulate pollution  
390 during haze events in China, *Nature*, 514, 218-222, 2014.

391 Jia, Y., Rahn, K. A., He, K., Wen, T., and Wang, Y.: A novel technique for quantifying the regional  
392 component of urban aerosol solely from its sawtooth cycles, *Journal of Geophysical Research*  
393 *Atmospheres*, 113, 6089-6098, 2008.

394 Liu, X. G., Li, J., Qu, Y., Han, T., Hou, L., Gu, J., Chen, C., Yang, Y., Liu, X., and Yang, T.:  
395 Formation and evolution mechanism of regional haze: a case study in the megacity Beijing,  
396 China, *Atmospheric Chemistry & Physics*, 13, 4501-4514, 2013.

397 Liu, Y., Gibson, E. R., Cain, J. P., Wang, H., Grassian, V. H., and Laskin, A.: Kinetics of  
398 heterogeneous reaction of CaCO<sub>3</sub> particles with gaseous HNO<sub>3</sub> over a wide range of humidity,  
399 *The Journal of Physical Chemistry A*, 112, 1561-1571, 2008.

400 Lv, L., Liu, W., Zhang, T., Chen, Z., Dong, Y., Fan, G., Xiang, Y., Yao, Y., Yang, N., and Chu, B.:  
401 Observations of particle extinction, PM<sub>2.5</sub> mass concentration profile and flux in north China  
402 based on mobile lidar technique, *Atmospheric Environment*, 2017.

403 Pan, X. L., Yan, P., Tang, J., Ma, J. Z., Wang, Z. F., Gbaguidi, A., and Sun, Y. L.: Observational  
404 study of influence of aerosol hygroscopic growth on scattering coefficient over rural area near  
405 Beijing mega-city, *Atmospheric Chemistry & Physics*, 9, 7519-7530, 2009.

406 Pilinis, C., Seinfeld, J. H., and Grosjean, D.: Water content of atmospheric aerosols, *Atmospheric*  
407 *Environment*, 23, 1601-1606, 1989.

408 Seinfeld, J. H., and Pandis, S. N.: *Atmospheric Chemistry and Physics: From Air Pollution to*  
409 *Climate Change*, John Wiley & Sons, USA, 1986.

410 Su, F., Gao, Q., Zhang, Z., REN, Z.-h., and YANG, X.-x.: Transport pathways of pollutants from  
411 outside in atmosphere boundary layer, *Research of Environmental Sciences*, 1, 26-29, 2004.

412 Sun, Y., Jiang, Q., Wang, Z., Fu, P., Li, J., Yang, T., and Yin, Y.: Investigation of the sources and  
413 evolution processes of severe haze pollution in Beijing in January 2013, *Journal of Geophysical*  
414 *Research: Atmospheres*, 119, 4380-4398, 2014a.

415 Sun, Y. L., Jiang, Q., Wang, Z. F., Fu, P. Q., Li, J., Yang, T., and Yin, Y.: Investigation of the sources  
416 and evolution processes of severe haze pollution in Beijing in January 2013, *J. Geophys. Res.-*  
417 *Atmos.*, 119, 4380-4398, 10.1002/2014jd021641, 2014b.

418 Wallace, J. M., and Hobbs, P. V.: *Atmospheric science : an introductory survey*, Elsevier, 2006.

419 Wang, G., Zhang, R., Gomez, M. E., Yang, L., Levy Zamora, M., Hu, M., Lin, Y., Peng, J., Guo, S.,  
420 Meng, J., Li, J., Cheng, C., Hu, T., Ren, Y., Wang, Y., Gao, J., Cao, J., An, Z., Zhou, W., Li, G.,  
421 Wang, J., Tian, P., Marrero-Ortiz, W., Secret, J., Du, Z., Zheng, J., Shang, D., Zeng, L., Shao,  
422 M., Wang, W., Huang, Y., Wang, Y., Zhu, Y., Li, Y., Hu, J., Pan, B., Cai, L., Cheng, Y., Ji, Y.,  
423 Zhang, F., Rosenfeld, D., Liss, P. S., Duce, R. A., Kolb, C. E., and Molina, M. J.: Persistent  
424 sulfate formation from London Fog to Chinese haze, *Proc Natl Acad Sci U S A*, 113, 13630-  
425 13635, 10.1073/pnas.1616540113, 2016.



426 Wang, H., Zhang, X., Gong, S., Chen, Y., Shi, G., and Li, W.: Radiative feedback of dust aerosols  
427 on the East Asian dust storms, *Journal of Geophysical Research*, 115, 6696-6705, 2010.

428 Wang, H., Shi, G. Y., Zhang, X. Y., Gong, S. L., Tan, S. C., Chen, B., Che, H. Z., and Li, T.:  
429 Mesoscale modeling study of the interactions between aerosols and PBL meteorology during  
430 a haze episode in China Jing-Jin-Ji and its near surrounding region - Part 2: Aerosols' radiative  
431 feedback effects, *Atmospheric Chemistry & Physics*, 15, 3277-3287, 2015a.

432 Wang, H., Xue, M., Zhang, X. Y., Liu, H. L., Zhou, C. H., Tan, S. C., Che, H. Z., Chen, B., and Li,  
433 T.: Mesoscale modeling study of the interactions between aerosols and PBL meteorology  
434 during a haze episode in Jing-Jin-Ji (China) and its nearby surrounding region – Part 1:  
435 Aerosol distributions and meteorological features, *Atmospheric Chemistry and Physics*, 15,  
436 3257-3275, 10.5194/acp-15-3257-2015, 2015b.

437 Wang, J., Wang, Y., Liu, H., Yang, Y., Zhang, X., Li, Y., Zhang, Y., and Deng, G.: Diagnostic  
438 identification of the impact of meteorological conditions on PM<sub>2.5</sub> concentrations in Beijing,  
439 *Atmospheric Environment*, 81, 158-165, 10.1016/j.atmosenv.2013.08.033, 2013a.

440 Wang, J., Wang, S., Jiang, J., Ding, A., Zheng, M., Zhao, B., Wong, D. C., Zhou, W., Zheng, G.,  
441 Wang, L., Pleim, J. E., and Hao, J.: Impact of aerosol–meteorology interactions on fine particle  
442 pollution during China’s severe haze episode in January 2013, *Environmental Research Letters*,  
443 9, 094002, 10.1088/1748-9326/9/9/094002, 2014a.

444 Wang, J. Z., Gong, S., Zhang, X. Y., Yang, Y. Q., Hou, Q., Zhou, C., and Wang, Y.: A parameterized  
445 method for air-quality diagnosis and its applications, *Advance of Meteorology*,  
446 doi:10.1155/2012/238589, 1-10, 2012.

447 Wang, X., Chen, J., Sun, J., Li, W., Yang, L., Wen, L., Wang, W., Wang, X., Collett, J. L., and Shi,  
448 Y.: Severe haze episodes and seriously polluted fog water in Ji'nan, China, *Sci. Total Environ.*,  
449 493, 133-137, 2014b.

450 Wang, Z., Li, J., Wang, Z., Yang, W., Tang, X., Ge, B., Yan, P., Zhu, L., Chen, X., and Chen, H.:  
451 Modeling study of regional severe hazes over mid-eastern China in January 2013 and its  
452 implications on pollution prevention and control, *Science China Earth Sciences*, 57, 3-13,  
453 2014c.

454 Wang, Z. B., Hu, M., Wu, Z. J., Yue, D. L., He, L. Y., Huang, X. F., Liu, X. G., and Wiedensohler,  
455 A.: Long-term measurements of particle number size distributions and the relationships with  
456 air mass history and source apportionment in the summer of Beijing, *Atmospheric Chemistry  
457 and Physics*, 13, 10159-10170, 10.5194/acp-13-10159-2013, 2013b.

458 Wei, P., Cheng, S. Y., Li, J. B., and Su, F. Q.: Impact of boundary-layer anticyclonic weather system  
459 on regional air quality, *Atmospheric Environment*, 45, 2453-2463,  
460 10.1016/j.atmosenv.2011.01.045, 2011.

461 Zhang, L., Sun, J. Y., Shen, X. J., Zhang, Y. M., Che, H., Ma, Q. L., Zhang, Y. W., Zhang, X. Y., and  
462 Ogren, J. A.: Observations of relative humidity effects on aerosol light scattering in the Yangtze  
463 River Delta of China, *Atmospheric Chemistry & Physics*, 15, 2853-2904, 2015a.

464 Zhang, R. H., Li, Q., and Zhang, R. N.: Meteorological conditions for the persistent severe fog and  
465 haze event over eastern China in January 2013, *Science China Earth Sciences*, 57, 26-35, 2014.

466 Zhang, R. Y., Wang, G. H., Guo, S., Zarnora, M. L., Ying, Q., Lin, Y., Wang, W. G., Hu, M., and  
467 Wang, Y.: Formation of Urban Fine Particulate Matter, *Chemical Reviews*, 115, 3803-3855,

468 10.1021/acs.chemrev.5b00067, 2015b.

469 Zhang, X., Sun, J., Wang, Y., Li, W., Zhang, Q., Wang, W., Quan, J., Cao, G., Wang, J., Yang, Y.,  
470 and Zhang, Y.: Factors contributing to haze and fog in China, *Chinese Science Bulletin*  
471 (Chinese Version), 58, 1178, 10.1360/972013-150, 2013.

472 Zhang, X. Y., Wang, Y. Q., Lin, W. L., Zhang, Y. M., Zhang, X. C., Gong, S., Zhao, P., Yang, Y. Q.,  
473 Wang, J. Z., and Hou, Q.: Changes of Atmospheric Composition and Optical Properties Over  
474 BEIJING—2008 Olympic Monitoring Campaign, *Bulletin of the American Meteorological*  
475 *Society*, 90, 1633–1651, 2009.

476 Zhang, X. Y., Wang, Y. Q., Niu, T., Zhang, X. C., Gong, S. L., Zhang, Y. M., and Sun, J. Y.:  
477 Atmospheric aerosol compositions in China: spatial/temporal variability, chemical signature,  
478 regional haze distribution and comparisons with global aerosols, *Atmos. Chem. Phys.*, 11,  
479 26571-26615, 2012.

480 Zhang, X. Y., Wang, J. Z., Wang, Y. Q., Liu, H. L., Sun, J. Y., and Zhang, Y. M.: Changes in chemical  
481 components of aerosol particles in different haze regions in China from 2006 to 2013 and  
482 contribution of meteorological factors, *Atmos. Chem. Phys.*, 15, 12935-12952, 10.5194/acp-  
483 15-12935-2015, 2015c.

484 Zheng, B., Zhang, Q., Zhang, Y., He, K. B., Wang, K., Zheng, G. J., Duan, F. K., Ma, Y. L., and  
485 Kimoto, T.: Heterogeneous chemistry: a mechanism missing in current models to explain  
486 secondary inorganic aerosol formation during the January 2013 haze episode in North China,  
487 *Atmospheric Chemistry and Physics*, 15, 2031-2049, 10.5194/acp-15-2031-2015, 2015a.

488 Zheng, G. J., Duan, F. K., Su, H., Ma, Y. L., Cheng, Y., Zheng, B., Zhang, Q., Huang, T., Kimoto,  
489 T., Chang, D., Poschl, U., Cheng, Y. F., and He, K. B.: Exploring the severe winter haze in  
490 Beijing: the impact of synoptic weather, regional transport and heterogeneous reactions,  
491 *Atmospheric Chemistry and Physics*, 15, 2969-2983, 10.5194/acp-15-2969-2015, 2015b.

492 Zhu, T., Shang, J., and Zhao, D. F.: The roles of heterogeneous chemical processes in the formation  
493 of an air pollution complex and gray haze, *Science China Chemistry*, 54, 145-153, 2011.

494

495 **Data Availability**

496 The data that support the findings of this study are available from the corresponding author upon  
497 reasonable request.

498

499 **Acknowledgements:**

500 This research is supported by the National Key Project of MOST (2016YFC0203306), the Atmospheric  
501 Pollution Control - the Prime Minister Fund, and the Basic Scientific Research Progress of the Chinese  
502 Academy of Meteorological Sciences (2016Z001).

503

504 **Author Contributions:**

505 X.Y.Z. and Y.Q.W. designed the research; X.Y.Z, J.T.Z and H.C.C carried out the analysis of observations.  
506 Y.S.D provided and analyzed laser radar data. Y.M.Z provided aerosol species data. J.Z.W provided  
507 PLAM data. J.T.Z. wrote the first manuscript and X.Y.Z. revised the manuscript. All authors read and  
508 approved the final version.

509

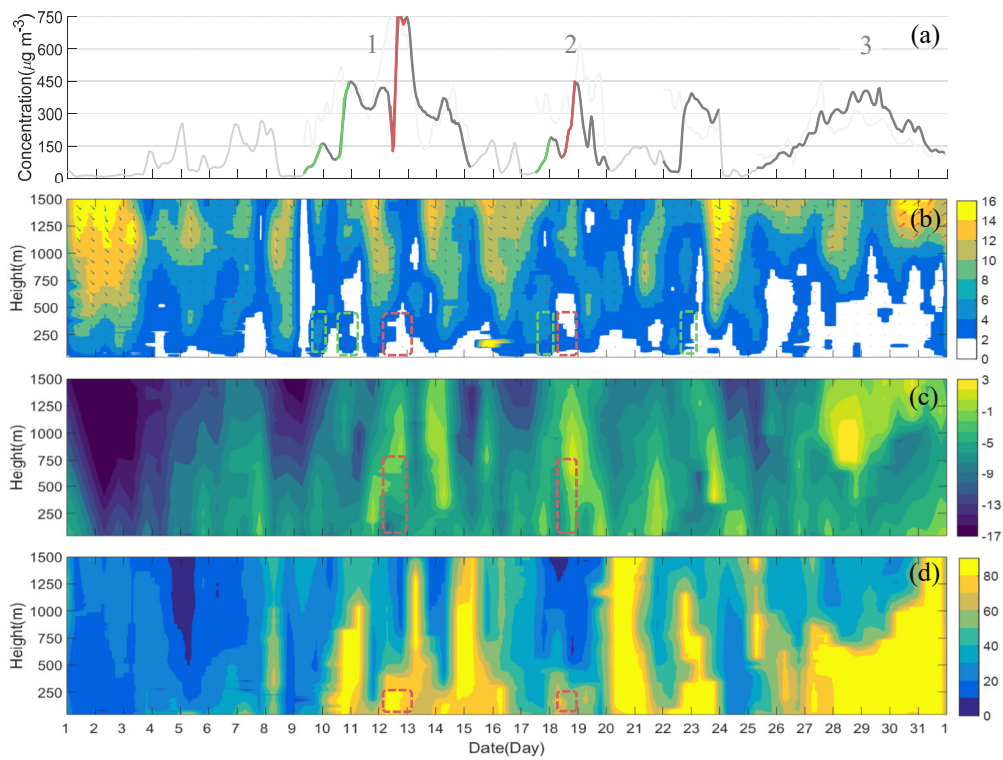
510 **Additional Information:**

511 **Competing financial interests:** The authors declare no competing financial interests.

512

513 **Figures**

514



515

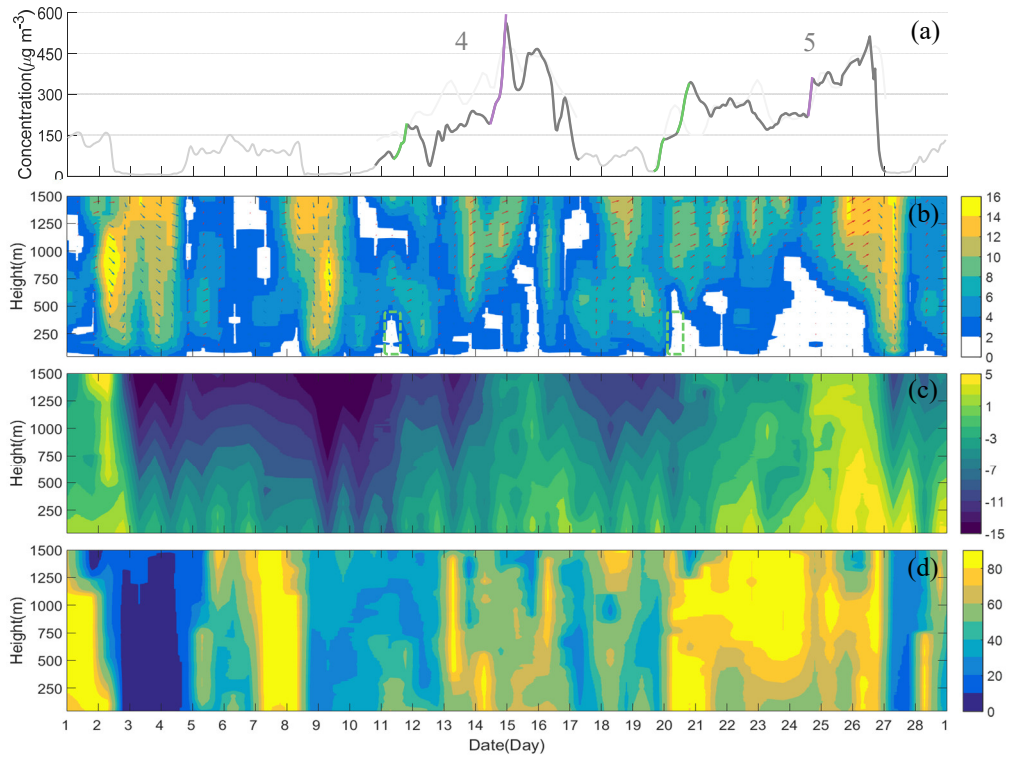
516 **Figure 1. Temporal variations in urban mean PM<sub>2.5</sub> and vertical distributions of meteorological factors in**

517 **January 2013. (a)PM<sub>2.5</sub> mass concentration (dark gray or gray: Beijing; light gray: Baoding); (b) winds (vectors;**

518 **red vectors: southwesterly winds) and wind velocity (shadings; units: m/s); (c)temperature (shadings; units:  $^{\circ}\text{C}$ );**

519 **(d)RH (shadings; units: %); (green boxes: rising processes; red boxes: cumulative explosive processes)**

520

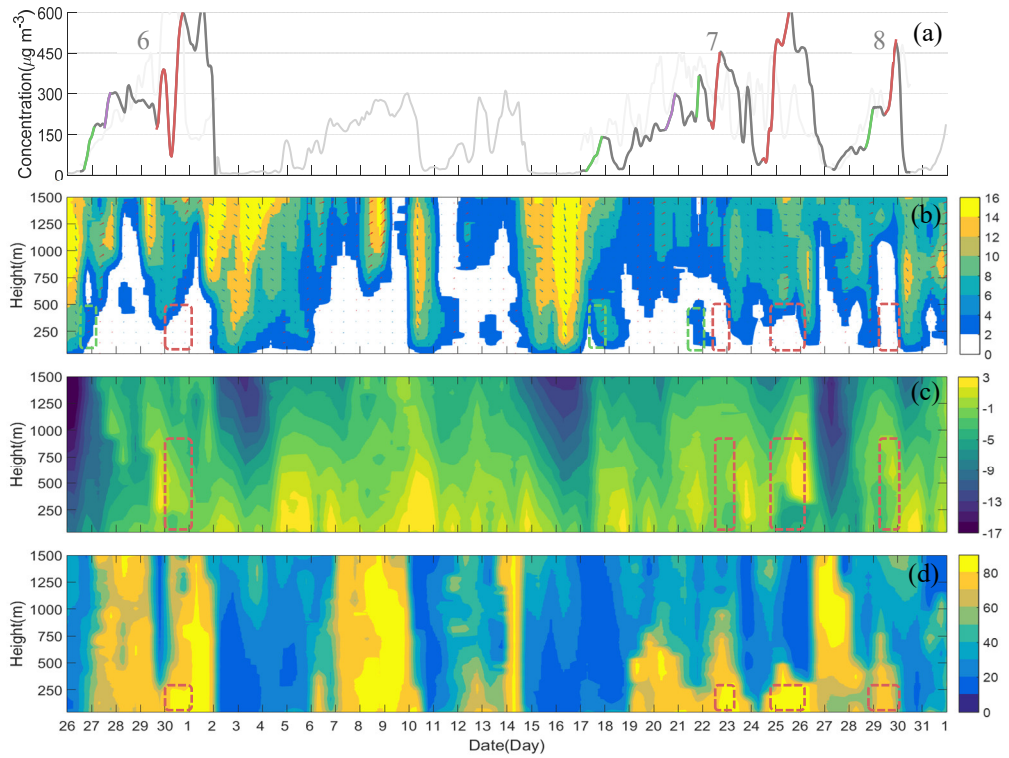


521

522 **Figure 2. Temporal variations in urban mean PM<sub>2.5</sub> and vertical distributions of meteorological factors in**  
 523 **February 2014.** (a)PM<sub>2.5</sub> mass concentration (dark gray or gray: Beijing; light gray: Baoding); (b) winds (vectors;  
 524 red vectors: southwesterly winds) and wind velocity (shadings; units: m/s); (c)temperature (shadings; units:°C);  
 525 (d)RH (shadings; units: %); (green boxes: rising processes)

526

527



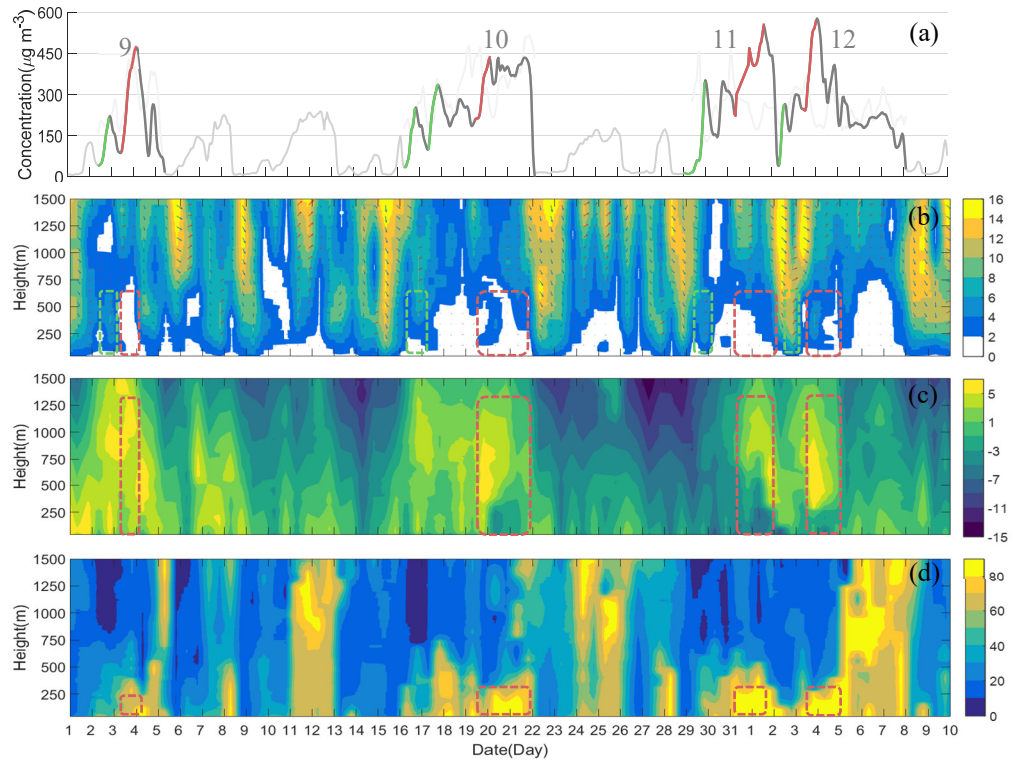
528

529 **Figure 3. Temporal variations in urban mean PM<sub>2.5</sub> and vertical distributions of meteorological factors in**  
 530 **December 2015. (a)PM<sub>2.5</sub> mass concentration (dark gray or gray: Beijing; light gray: Baoding); (b) winds (vectors;**  
 531 **red vectors: southwesterly winds) and wind velocity (shadings; units: m/s); (c)temperature (shadings; units:  $^{\circ}\text{C}$ );**  
 532 **(d)RH (shadings; units: %); (green boxes: rising processes; red boxes: cumulative explosive processes)**

533

534

535



536

537

**Figure 4. Temporal variations in urban mean PM<sub>2.5</sub> and vertical distributions of meteorological factors in**

538

**December 2016. (a)PM<sub>2.5</sub> mass concentration (dark gray or gray: Beijing; light gray: Baoding); (b) winds (vectors;**

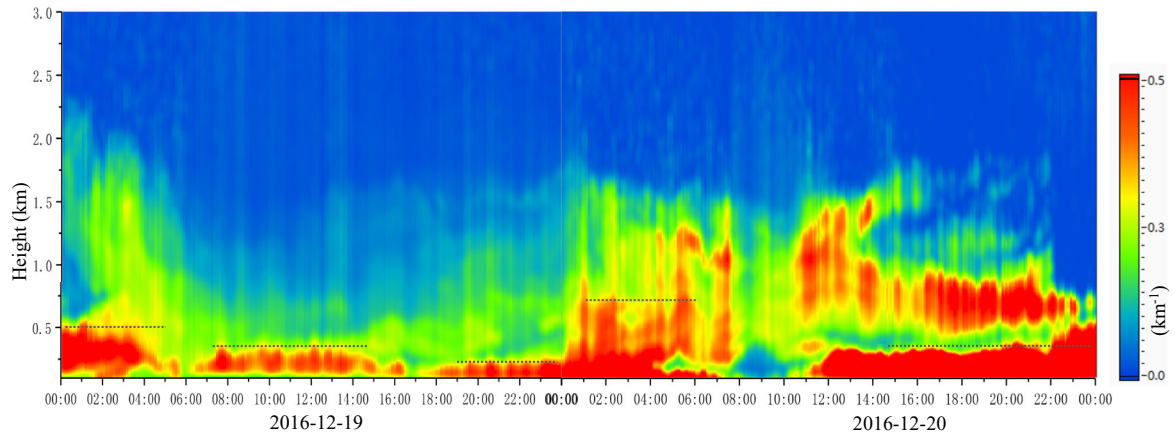
539

**red vectors: southwesterly winds) and wind velocity (shadings; units: m/s); (c)temperature (shadings; units:°C);**

540

**(d)RH (shadings; units: %); (green boxes: rising processes; red boxes: cumulative explosive processes)**

541



542

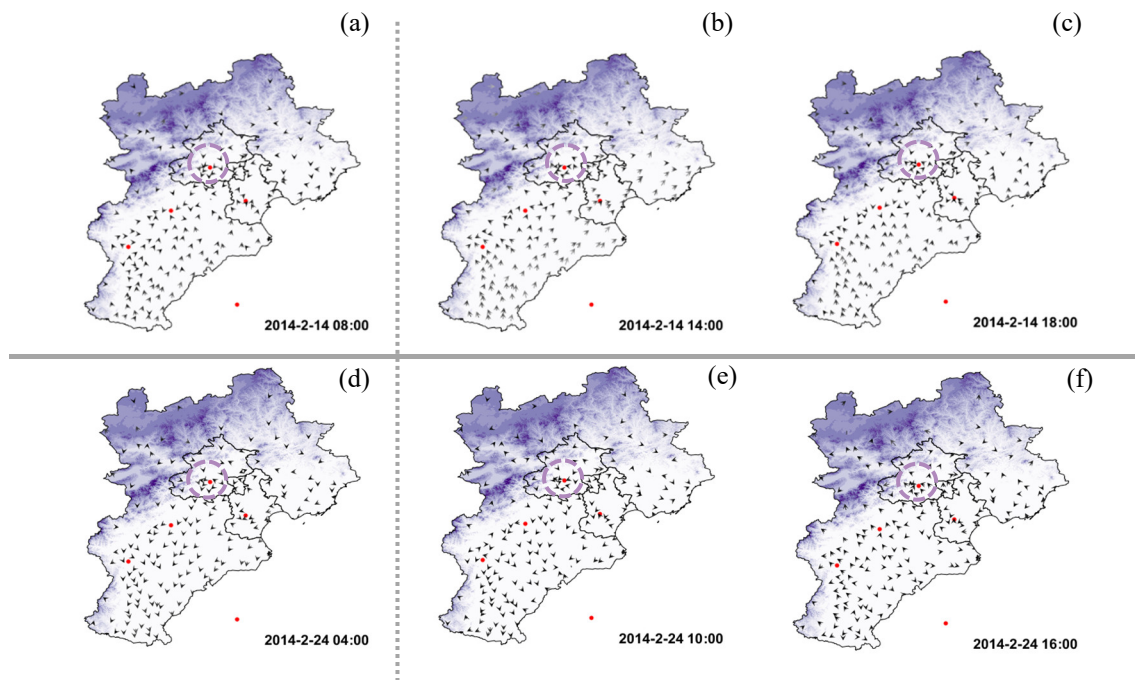
543

544

545

**Figure 5. Time series of vertical distributions of the extinction coefficient of aerosols observed in the northern urban area of Beijing from 19 to 20 December 2016 (The dashed lines: the approximate boundary layer height)**

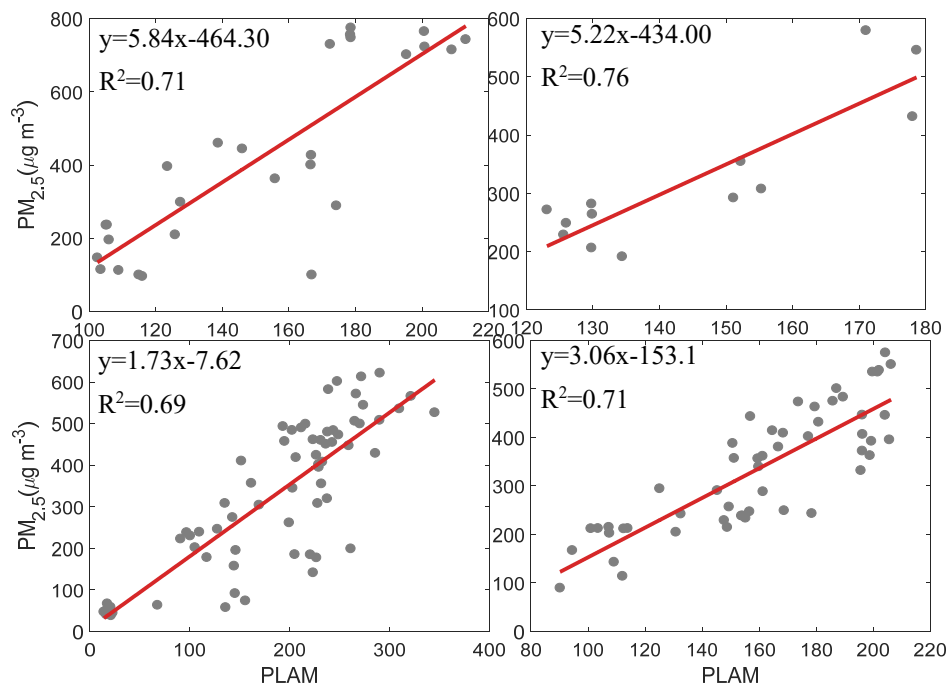




546

547 **Figure 6. Surface wind distributions before (a, d) and during (b, c; d, e) two convergent explosive growth**  
 548 **processes in February 2014 on the North China Plain.**

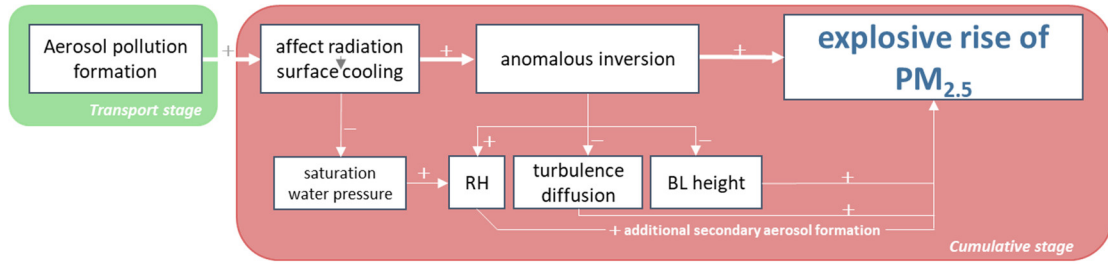
549



551

552 **Figure 7. Correlation between PLAM and PM<sub>2.5</sub> during the cumulative explosive growth processes in**553 **January 2013 (a) , December 2015 (c), December 2016 (d) respectively, and the convergent explosive growth**554 **processes in February 2014 (b).**

555



556

557 **Figure 8. A schematic figure of the formation mechanism for winter heavy pollution episodes in Beijing, which**

558 **consist of the transport stage (green background) and the cumulative stage (red background).**